7614 *Biochemistry* **2009,** *48,* 7614–7620
DOI: 10.1021/bi900813x

BIOCHEMISTRY
including biophysical chemistry & molecular biology
Article

Discovery of Inhibitors of Lupin Diadenosine 5′,5‴-P^1,P^4-Tetraphosphate Hydrolase by Virtual Screening[†]

Kim M. Branson,[‡,§,#] Haydyn D. T. Mertens,[∥,#] James D. Swarbrick,[∥] Jamie I. Fletcher,[∥] Lukasz Kedzierski,[⊥] Kenwyn R. Gayler,[∥] Paul R. Gooley,[∥] and Brian J. Smith*[,‡]

[‡]*Structural Biology Division, The Walter and Eliza Hall Institute of Medical Research, Parkville, Victoria 3052, Australia,* [§]*Department of Medical Biology and* [∥]*Department of Biochemistry and Molecular Biology, Bio21 Molecular Science and Biotechnology Institute, The University of Melbourne, Parkville, Victoria 3010, Australia, and* [⊥]*Infection and Immunity Division, The Walter and Eliza Hall Institute of Medical Research, Parkville, Victoria 3052, Australia.* [#]*These authors contributed equally.*

Received May 11, 2009; Revised Manuscript Received July 14, 2009

ABSTRACT: Novel inhibitors of lupin diadenosine 5′,5‴-P^1,P^4-tetraphosphate (Ap_4A) hydrolase have been identified by *in silico* screening of a large virtual chemical library. Compounds were ranked on the basis of a consensus from six scoring functions. From the top 100 ranked compounds six were selected and initially screened for inhibitory activity using a single concentration isothermal titration calorimetry assay. Two of these compounds that showed excellent solubility properties were further analyzed, but only one [NSC51531; 2-((8-hydroxy-4-(4-methyl-2-sulfoanilino)-9,10-dioxo-9,10-dihydro-1-anthracenyl)amino)-5-methylbenzenesulfonic acid] exhibited competitive inhibition with a K_i of 1 μM. A structural analogue of this compound also exhibited competitive inhibition with a comparable K_i of 2.9 μM. ^{1}H, ^{15}N NMR spectroscopy was used to map the binding site of NSC51531 on lupin Ap_4A hydrolase and demonstrated that the compound bound specifically in the substrate-binding site, consistent with the competitive inhibition results. Binding of NSC51531 to the human form of Ap_4A hydrolase is nonspecific, suggesting that this compound may represent a useful lead in the design of specific inhibitors of the plant-like form of Ap_4A hydrolases.

Diadenosine 5′,5‴-P^1,P^4-tetraphosphate (Ap_4A)[1] has wide ranging physiological roles in both prokaryotes and eukaryotes (*1*, *2*). In human physiology Ap_4A has a pivotal role in vasoconstriction and myocardial function, acting as both a cellular signaling molecule and a second messenger in the regulation of gene expression (*3*). In bacterial systems Ap_4A appears to have intracellular signaling roles involved in the regulation of invasion and bacterial pathogenesis (*4*−*6*).

All cells produce Ap_4A under normal physiological conditions, and the cellular systems for its degradation are ubiquitously expressed (*7*). Ap_4A (and related dinucleotide polyphosphates) is typically degraded by nucleotide hydrolases that asymmetrically cleave Ap_4A to yield ATP (adenosine triphosphate) and AMP (adenosine monophosphate) (*8*, *9*). These asymmetrically cleaving Ap_4A hydrolases have been identified in plants, animals, protozoa, and proteobacteria, and all are members of the Nudix hydrolase family. The animal and plant Ap_4A hydrolases have little sequence similarity apart from the Nudix motif, while the bacterial enzymes show greater similarity to the plant enzymes than to their animal counterparts (*4*). Notably, of the 15 residues identified to be involved in ligand binding in the plant Ap_4A hydrolase structure (*10*), 10 are strictly conserved and 4 are conservative substitutions between the plant and bacterial enzymes. The plant hydrolase will therefore likely serve as a useful model for the bacterial and parasitic enzymes. The plant-like hydrolases (conserved domain cd03671) include those from the potentially fatal human parasites *Trypanosoma brucei* (gi|62360166), responsible for African sleeping sickness, *Trypanosoma cruzi* (gi|70872560), the causative agent of Chagas disease, and *Leishmania major* (gi|68128542), the pathogen causing leishmaniasis.

The development of inhibitors of Ap_4A hydrolases may therefore have significant utility. Inhibitors of bacterial Ap_4A hydrolase may represent a novel class of antimicrobial agents. Disruption of the cellular signaling controlled by Ap_4A in pathogenic bacteria may reduce microbial pathogenesis during an infection. Methylene, halomethylene, and polyol derivatives of Ap_4A (*11*−*13*) are known competitive inhibitors of human, bacterial, and plant Ap_4A hydrolase. Suramin has also been reported to inhibit rodent Ap_4A hydrolase (*14*).

We report here the discovery of several novel small-molecule inhibitors of Ap_4A hydrolase from *Lupinus angustifolius* discovered using *in silico* screening. This success in identifying a

[†]This study was supported by a National Health and Medical Research Council grant. Infrastructure support from the NHMRC IRIIS (361646) and the Victorian State government OIS grants is gratefully acknowledged.

*To whom correspondence should be addressed. Telephone: (613) 9345-2687. Fax: (613) 9347-0852. E-mail: bsmith@wehi.edu.au.

[1]Abbreviations: Ap_4A, diadenosine 5′,5‴-P^1,P^4-tetraphosphate; HSQC, heteronuclear single-quantum correlated; NMR, nuclear magnetic resonance; ATP, adenosine triphosphate; AMP, adenosine monophosphate; PDB, Protein Data Bank; NCI DTP, National Cancer Institute Developmental Therapeutics Program; ITC, isothermal titration calorimetry; NSC51531, 2-((8-hydroxy-4-(4-methyl-2-sulfoanilino)-9,10-dioxo-9,10-dihydro-1-anthracenyl)amino)-5-methylbenzenesulfonic acid; NSC86169, 1,4-dihydroxy-5,8-di(4-toluidino)anthra-9,10-quinone; NSC89768, 3,4,9,10-perylenetetracarboxylic acid; NSC-113427, 2,2′-(4-(4,7-diamino-2-phenylpteridin-6-yl)phenazinediyl)diethanol; NSC133815, 2,2′-bicinchonic acid; NSC232476, 4-amino-*N*-(4-(2-hydroxyphenyl)-6-phenyl-2-pyrimidinyl)benzenesulfonamide; NSC300513, 5-hydroxy-1,4-di(4-toluidino)anthra-9,10-quinone; NSC305522, 8,11-dihydroxynaphtho[2,3-*b*]phenazine-7,12-dione; NSC401611, 5-methyl-2-((4-(methylamino)-9,10-dioxo-9,10-dihydro-1-anthracenyl)amino)benzenesulfonic acid.

 Published on Web 07/15/2009

high-affinity inhibitor of lupin Ap_4A hydrolase demonstrates the potential to identify inhibitors of bacterial and parasitic Ap_4A hydrolases with potential human therapeutic applications.

EXPERIMENTAL PROCEDURES

Virtual Screening. Virtual screening was performed using the DOCK (4.0.1) program (*15*). Docking spheres were generated using the SPHGEN utility. Energy and bump grids were calculated using the GRID program at a resolution of 0.35 Å; a dielectric of 4.0*r* and distance cutoff of 10.0 Å were used to evaluate the electrostatic components of the energy, and a 6-12 potential was used for the Lennard-Jones function. Flexible ligand docking was performed using the automated matching procedure for sampling ligand orientation, torsion drive and minimization methods for conformational searching, and energy optimization.

The Open NCI Database (October 2000 release) was converted from sdf format to three-dimensional SYBYL mol2 format using the Concord program (*16*). Gasteiger partial atomic charges were assigned, and each molecule was minimized using SYBYL (version 6.7; Tripos Inc., St. Louis, MO). After removal of molecules incompatible with the docking methods, the virtual library consisted of ~120000 entries.

The structure of lupin Ap_4A hydrolase in complex with ATP (PDB accession code 1JKN, model number 17) with ligand removed was used for virtual screening (*10*). Protons were added to fill unsatisfied valencies, and Kollman all-atom charges were assigned using the BIOPOLYMER module of SYBYL. Proton positions were minimized (200 iterations of conjugate gradient) with all other atoms held fixed.

The interaction energy between ligand and protein was evaluated using six different scoring functions, DOCK (*15*), SCORE (*17*), PMF (*18*), ChemScore (*19*, *20*), SMoG (*21*, *22*), and AutoDock (*23*), using our in-house SCORER program. The top-scoring 25 poses from the DOCK calculation were rescored using all six scoring functions. The representative pose for each ligand was chosen based on a product-of-ranks consensus analysis of these scores (*24*, *25*). A consensus ranking of all the compounds in the database was obtained from a principle-component consensus of the six scoring functions. The principle-component consensus uses a sum-of-ranks consensus where each scoring function is weighted by the eigenvector components of the principle eigenvalue of the matrix of rank correlations between all scoring functions (Branson and Smith, manuscript in preparation).

From the highest 100 ranked compounds, those compounds with a calculated log *P* greater than 3 were excluded from further consideration. The XlogP program (*26*) was used for predicting octanol/water partition coefficients (log *P*).

Isothermal Titration Calorimetry. The hydrolysis of Ap_4A by the lupin Ap_4A hydrolase enzyme was determined using an ITC-based method (*27*). Reactions were carried out using a VP-ITC isothermal titration calorimeter (Microcal) at a temperature of 25 °C, and data were collected and analyzed using the manufacturer supplied ORIGIN 6.0 software (OriginLab Corp.) and the software package GRACE. Both a single injection continuous kinetic assay and a multiple injection kinetic assay were conducted using a stirring speed of 310 rpm. For the continuous assay, reactions were started with a single 5 μL injection of Ap_4A (4.7 mM) into the sample cell (volume, 1.41 mL) containing the enzyme (5.3 nM), and the reaction was followed to completion. For the multiple injection method, 2.5−5.1 nM enzyme in the reaction cell was titrated with 20−40 $\times$2−3 μL injections of Ap_4A (1.0 mM) using a 60 s delay between successive injections. The apparent enthalpy (ΔH_{app}) for the hydrolysis of Ap_4A by the lupin enzyme was determined in a separate experiment in which 10 $\times$ 14 μL injections of ligand (1 mM) into either buffer alone or buffer containing enzyme (50.5 nM) were made using a 250 s spacing. ΔH_{app} was determined by integration of the thermogram corrected for heats of dilution. Buffer solution was carefully matched in both the ligand and enzyme solutions and consisted of 100 mM Tris−acetate, pH 7.7, 5 mM magnesium acetate, and 5% DMSO, and samples were degassed prior to the assay. Buffer solution, including DMSO, was shown not to inhibit enzyme activity. Inhibitor concentrations in the sample cell are as indicated in the text.

NMR Interaction Assay. Samples of ^{15}N-labeled lupin Ap_4A hydrolase were titrated with the compound NSC51531, and changes to peak intensity or chemical shift were monitored in 2D ^{15}N, ^{1}H HSQC spectra. The protein was expressed, purified, and prepared as previously described − the ^{1}H, ^{13}C, and ^{15}N resonances of the enzyme have been previously assigned (*28*). To assess the specificity of NSC51531 for the lupin Ap_4A hydrolase, a similar titration against the ^{15}N-labeled human Ap_4A hydrolase (E63A) was performed. The enzyme was expressed and purified as previously reported (*29*). The inactive E63A mutant is more stable to precipitation than wild type but binds substrate similarly to wild type.

Stock solutions of NSC51531 were prepared from 50 μL of DMSO to produce a 50 mM stock. NMR samples (0.22 mM lupin Ap_4A hydrolase, 0.25 mM human Ap_4A hydrolase) containing 20 mM [^{2}H]imidazole (pH 6.5), 20 mM $MgCl_2$, 0.02% NaN_3, and 90% H_2O/10% $^{2}H_2O$ were prepared in 550 μL and titrated to an equivalent concentration of ligand with the addition of 10 μL of DMSO. The NMR experiments were carried out at 25 °C using a Varian 500 or 600 MHz Inova spectrometer equipped with a 5 mm ^{1}H, ^{13}C, ^{15}N single *z*-axis gradient probe. Data were processed using NMRPipe (*30*) and subsequently analyzed in XEASY (*31*). ^{1}H chemical shifts were referenced to DSS at 0.0 ppm; ^{13}C and ^{15}N chemical shifts were calculated from the ^{1}H spectrometer frequency. Structural images were prepared using the PyMol program (DeLano Scientific LLC).

Cell Viability Assay. Primary human foreskin fibroblasts (a gift from Dr. Christopher Tonkin, WEHI) were maintained in DME medium containing 10% heath inactivated fetal bovine serum at 37 °C in 5% CO_2. The CellTiter Blue cell viability assay (Promega, Madison, WI) was used to determine compound toxicity as previously described (*32*). Briefly, compounds were dissolved in DMSO at 10 mM working concentration and titrated across the range of compound concentrations (2-fold dilutions from 100 μM to 49 nM) in culture media. The assay was set up in triplicate in 96-well plates with 10^3 cells/well. Cell viability was assessed spectrophotometrically at 550 nm with the reference wavelength of 630 nm. DMSO control was included in the assay. Readings were compared to the nontreated control, and the percent growth inhibition was calculated.

RESULTS

In Silico Screening. From the top-ranked 100 compounds selected by consensus rescoring only 7 compounds had a predicted log *P* of *less than* 3; this cutoff value for log *P* was

considered a reasonable predictor of water solubility. Of these 7 compounds, all but 1 was available from the NCI Developmental Therapeutics Program (NCI DTP). Thus, six compounds (NSC51531, NSC89768, NSC113427, NSC133815, NSC232476, and NSC305522) were initially assayed for inhibition of lupin Ap_4A hydrolase using ITC.

Hydrolysis of Ap_4A by Lupin Ap_4A Hydrolase. The activity of the wild-type Ap_4A hydrolase was determined using ITC. The apparent enthalpy, ΔH_{app}, for the hydrolysis of Ap_4A by the wild-type lupin Ap_4A hydrolase enzyme was determined to be -123 kJ mol^{-1}. The kinetic constants, K_m and k_{cat}, were determined from a nonlinear least-squares fit of the calorimetric profile generated during replicate multiple injection kinetic assays to the standard Michaelis–Menten equation (Figure 1) and were 2.72 ± 0.49 μM and 10.15 ± 0.56 s^{-1}, respectively. These values are similar to those previously determined by other methods (*33*).

Inhibition of Lupin Ap_4A Hydrolase. Six compounds from the NCI DTP were initially screened for inhibition of the Ap_4A hydrolysis reaction using ITC. A first-pass screen was conducted using the single injection continuous assay and potential inhibition of the hydrolysis reaction identified from thermograms exhibiting an increased time to return to baseline relative to the enzyme reaction in the absence of inhibitor (Figure 2a). Three compounds, NSC113427, NSC133815, and NSC305522, did not exhibit any enzyme inhibition at concentrations in excess of 100 μM. The remaining three compounds, NSC51531, NSC89768, and NSC232476, were soluble in 5% DMSO (Table 1) and were observed to inhibit the enzyme. The molecular structures of these compounds are presented in Figure 3. NSC89768 was poorly soluble and was excluded from the subsequent analysis where accurate inhibitor concentrations were required for estimation of the apparent K_i. From visual inspection of the thermograms from the continuous assays compound NSC51531, possessing a 1,4-diaminoanthracene-9,10-dione core, exhibited the most potent inhibition of the three compounds identified.

Compounds NSC86169, NSC30051, and NSC401611 are clear structural analogues of NSC51531, containing the 1,4-diaminoanthracene-9,10-dione core (Figure 3); these compounds were also obtained from the NCI DTP. The analogues NSC86169 and NSC300513 were poorly soluble in 5% DMSO (Table 1); however, inhibition was observed at relatively high concentrations in the ITC assays. In contrast, NSC401611 was readily soluble in 5% DMSO and showed inhibition of the single injection assay. Inhibition constants for NSC51531, NSC232476, and NSC401661 were subsequently determined using a multiple injection assay. The predicted log *P* of NSC401611 was 3.0 and narrowly missed being included in the initial selection of compounds.

Determination of Inhibition Constants. A multiple injection ITC method was used to determine inhibition constants for NCI compounds NSC51531, NSC232476, and NSC401611. Under pseudo-first-order and steady-state conditions, the rate of reaction for a series of substrate concentrations was obtained from the measured thermal power following each injection. The inhibition constants (K_i) were derived from a nonlinear least-squares fit of the multiple injection ITC data to the Michaelis–Menten equation for competitive inhibition (*1*):

$$v = \frac{k_{cat}[E][S]_t}{K_M\left(1+\frac{[I]}{K_i}\right)+[S]_t} \quad (1)$$

where v is the reaction velocity; [E], [I], and [S] are the concentrations of enzyme, inhibitor, and substrate at a given

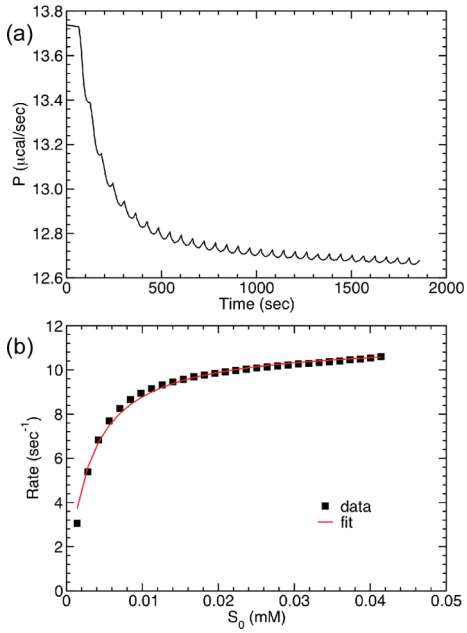

FIGURE 1: Calorimetric thermogram and Michaelis–Menten curve for Ap_4A hydrolysis. (a) Raw data for the multiple injection method are shown for 40×2 μL sequential injections of Ap_4A (1.0 mM) into a sample cell containing the lupin Ap_4A hydrolase (2.5 nM) at 25 °C. An initial delay of 60 s and a spacing of 60 s between injections were applied. (b) The change in thermal power was converted to rate and fit using ORIGIN 6.0 software and was corrected for enzyme dilution.

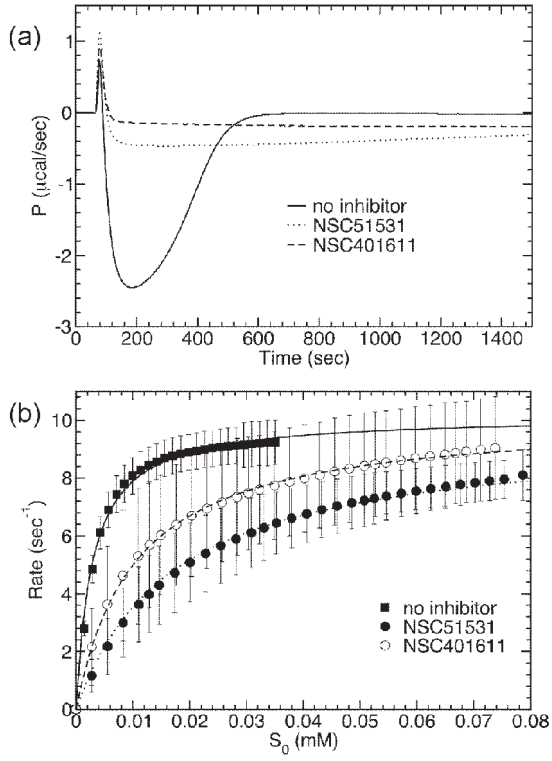

FIGURE 2: Inhibition of Ap_4A hydrolysis. (a) 5.3 nM lupin Ap_4A hydrolase in 100 mM Tris–acetate, pH 7.7, 5 mM magnesium acetate, and 5% DMSO was equilibrated at 25 °C in the presence or absence of potential inhibitors (see Table 1 for compound concentrations). Reaction was started with a single 5 μL injection of Ap_4A (4.7 mM). (b) Michaelis–Menten curves constructed from multiple injection ITC data using ORIGIN 6.0 for lupin Ap_4A hydrolase (2.5 nM) hydrolysis of Ap_4A (1.0 mM) in the presence of inhibitors (see Table 2 for compound concentrations).

Table 1: Assay Conditions and Properties of the NCI Compounds That Inhibited Lupin Ap_4A Hydrolase[a]

compound	concn (μM)[b]	solubility	rank[c]	inhibition[d]
		In Silico Screening Predictions		
NSC51531	100	good	6	+
NSC133815	< 539	poor	54	−
NSC89768	< 356	poor	65	+
NSC305522	< 428	very poor	87	−
NSC232476	341	good	93	+
NSC113427	171	good	99	−
		Structural Analogues		
NSC401611	223	good	73	+
NSC86169	< 232	very poor	691	+
NSC300513	< 272	poor	2026	+
DMSO	5% (w/v)	N/A	N/A	−

[a] Inhibition was measured as an increase in the time for the calorimetric signal to return to baseline relative to the wild-type enzyme without inhibitor added. [b] Concentration was dependent on compound solubility in 5% DMSO. Where the solubility was poor, only an upper limit of the concentration was available. [c] Rank from the consensus scoring of the six scoring functions described. [d] (+) indicates inhibition; (−) indicates no observed inhibition.

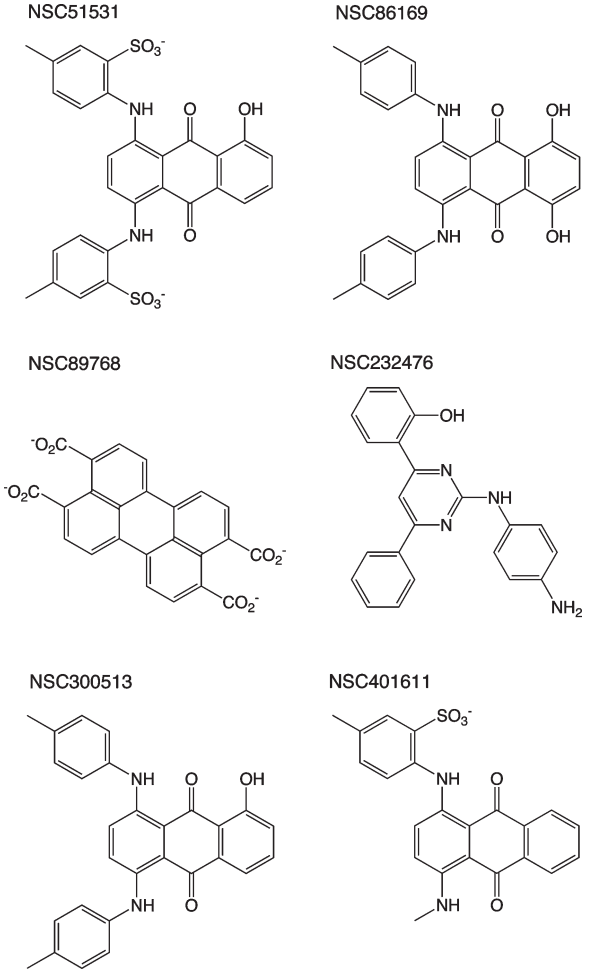

FIGURE 3: Chemical structures of inhibitors of lupin Ap_4A hydrolase. NSC51531, NSC89768, and NSC232476 were identified through *in silico* screening. NSC86169, NSC300513, and NSC-401611 are structural analogues of NSC51531.

Table 2: Inhibition Constants from Multiple Injection Assay

compound	concn[a]	K_i (μM)[b]	k_{cat} (s^{-1})[b,c]
NSC51531	4.8	1.09 ± 0.29	10.14 ± 0.56
NSC232476[d]	6.8	~5	~12
NSC401611	4.5	2.89 ± 2.06	10.54 ± 0.24

[a] Final concentration in sample cell (μM). [b] Reported values are the mean of three replicate determinations and the standard deviation. [c] k_{cat} and K_m constrained during fitting procedure within experimental errors. [d] Data for this compound could not be adequately fit to simple competitive inhibition.

time t, respectively; and k_{cat}, K_M, and K_i are the catalytic, Michaelis−Menten, and inhibition rate constants, respectively.

Figure 2b shows the reaction rates at each substrate concentration for the enzyme alone (no inhibitor) and in the presence of NSC51531 or NSC401611, fit to eq 1. The K_is for the three inhibitors, determined from the fits, are presented in Table 2.

NMR ^{15}N Chemical Shift Perturbation. The compound exhibiting the greatest inhibition, NSC51531, was tested for its ability to bind the Ap_4A binding site of the enzyme. Titration of ^{15}N-labeled lupin Ap_4A hydrolase with NSC51531 caused only small chemical shift changes but markedly broadened a number of resonances, indicating that the binding of ligand was in the intermediate exchange regime (*34*). Figure 4a shows a histogram plot of the intensity changes at 1:1 enzyme to ligand ratio. The most significant intensity changes were mapped onto the structure of the protein in Figure 4b. These changes are localized to helix II, the N-terminal end of helix IV, and the strands of the five-stranded β-sheet and are consistent with the binding of NSC51531 to the Ap_4A binding site (*10*, *35*). Compound NSC51531 may therefore inhibit Ap_4A hydrolase by competing for substrate binding.

Titration of ^{15}N-labeled human Ap_4A hydrolase (E63A) with NSC51531 also broadened a number of resonances. A histogram plot of the intensity changes at 1:1 enzyme to ligand and mapping the most significant intensity changes onto the structure are shown in Figure 5. In this case, while several resonances (H42, E135) near the ligand binding site were broadened, a number of resonances distant from the binding site were also affected, suggesting that NSC51531 is less specific in its interaction with this form of the enzyme. Substrate is expected to sandwich between Y87 and F133; however, the resonances of Y87 and its flanking residues were not affected. The NH of F133 is broad prior to the addition of ligand. The resonances of K137 and its flanking residues, which are distant from the binding site, are markedly broadened, suggesting nonspecific binding to the human enzyme.

Toxicity of NSC51531. The effect of NSC51531 on human fibroblasts was examined to determine the potential toxicity against mammalian cells. NSC51531 was incubated with human fibroblasts for 24 h, after which the effect on cell growth was assayed. No effect on cell viability or growth was detected at concentrations up to 100 μM (Figure 6).

DISCUSSION

Virtual screening has identified several novel small molecule inhibitors of lupin Ap_4A hydrolase with K_i values in the low micromolar range. This is the first successful application of virtual screening to an Ap_4A hydrolase. Three of the six compounds received from the NCI exhibited inhibition of the

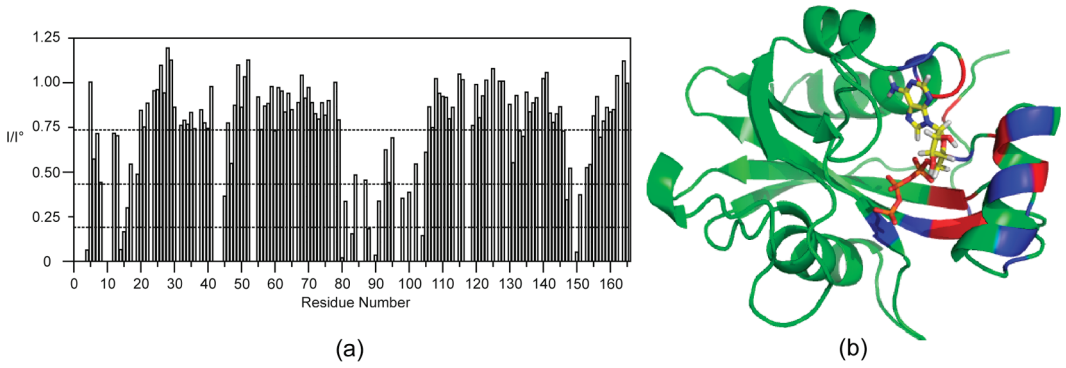

FIGURE 4: NMR titration of ^{15}N-labeled lupin Ap_4A hydrolase with NSC51531. (a) Histogram plot of relative intensity of the ^{15}NH resonances in the absence of NSC51531 ($I°$) versus the presence of a molar equivalent of NSC51531 (I). The mean intensity and standard deviation are 0.746 ± 0.282. Dashed lines represent the mean and one and two standard deviations. Residues L3, E11, G18, N23, A31, M42, Q44, R54, G66, Y82, R89, L92, W96, G97, D99, K101, G114, Q117, E118, D124, and S126 were excluded due to resonance overlap. Proline residues are in positions 9, 10, 37, 43, 77, 85, 86, 129, 139, 152, and 163. (b) Structure of Ap_4A hydrolase. Green indicates no significant broadening, blue within one to two standard deviation, and red more than two standard deviations of the mean intensity. The ligand ATP is presented to indicate the location of the enzyme active site; the largest perturbations are localized about the enzyme active site.

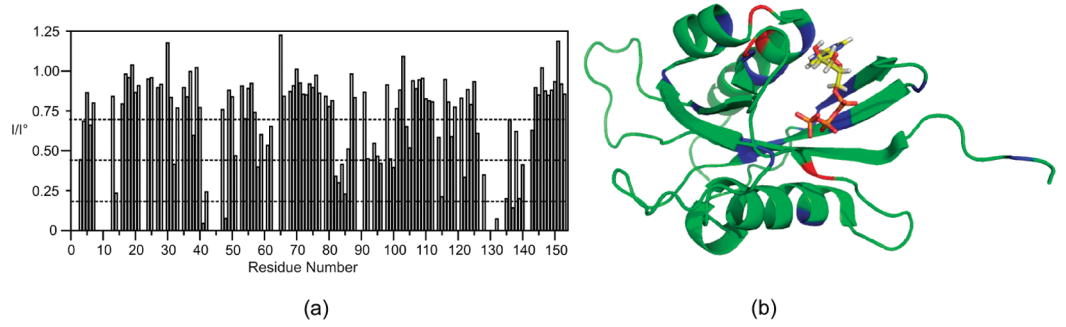

FIGURE 5: NMR titration of ^{15}N-labeled human Ap_4A hydrolase with NSC51531. (a) Histogram plot of relative intensity of the ^{15}NH resonances in the absence of NSC51531 ($I°$) versus the presence of a molar equivalent of NSC51531 (I). The mean intensity and standard deviation are 0.719 ± 0.266. Dashed lines represent the mean and one and two standard deviations. Residues L8, R9, A10, C11, G12, I15, K23, N26, I29, L34, W43, T44, A60, A63, T64, E67, I78, R90, I97, S113, R120, A127, Q129, L130, A131, F133, K134, Q141, and E142 were excluded due to resonance overlap or the peak in the absence of ligand was very weak. Proline residues are in positions 22, 45, 46, 52, and 93. (b) Structure of human Ap_4A hydrolase. Green indicates no significant broadening, blue within one to two standard deviation, and red more than two standard deviations of the mean intensity.

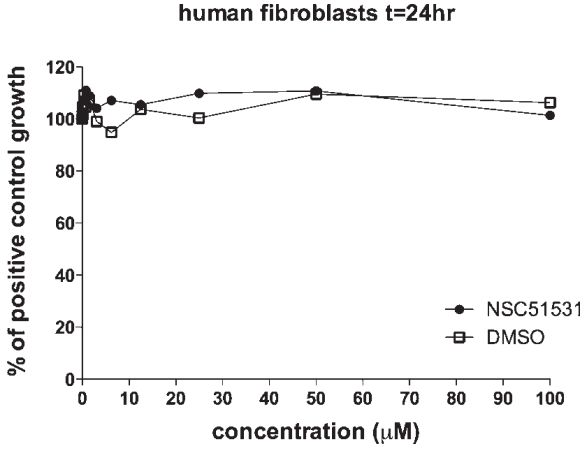

FIGURE 6: Toxicity of NSC51531 against human fibroblasts. Inhibition of cell growth after 24 h incubation with NSC51531 and DMSO, corrected against a nontreated control.

enzyme. The most active of these, NSC51531, was ranked number 6 in the initial rank-ordered list of ~120000 compounds and was the highest ranked compound with a log P less than 3. Reiterating, NSC51531 was the highest ranked compound we considered suitable for testing.

Comparison of the docked pose of NSC51531 with the original NMR complex of Ap_4A hydrolase with ATP−MgF_x (*10*), combined with the NMR titration analysis (Figure 4), indicates that the compound occupies the binding site in a very similar manner to ATP (Figure 7). The naphthalene group occupies the same space as the adenine ring of ATP, flanked by the hydrophobic side chains of I36, A39, V88, V147, and F149. The naphthyl−hydroxyl forms a hydrogen bond with the NH_3^+ group of the side chain of K150. One of the sulfonate groups of NSC51531 is in close proximity to K58 on the surface of the protein, while the second sulfonate group forms an interaction with the guanadinium group of R33; this latter sulfonate lies close to where the furan-linked phosphate of ATP lies (in the NMR structure of the complex of Ap_4A hydrolase with ATP−MgF_x). The side-chain groups of several other residues of the hydrolase contact NSC51531, including F84, K91, L92, and W96.

NSC51531 and NSC401611 have comparable affinities to the previously reported substrate analogue di(adenosine-5-*O*-phosphorothio)erythritol that inhibits lupin Ap_4A hydrolase with a K_i of 1.5 μM. The substrate analogues also inhibit the human form of the hydrolase (K_i of 0.5 μM) (*12*). Although NSC51531 interacts with human Ap_4A hydrolase, it also appears to interact nonspecifically. The solution structure of human Ap_4A hydrolase (*29*) and the crystal structure of *Caenorhabditis elegans* Ap_4A

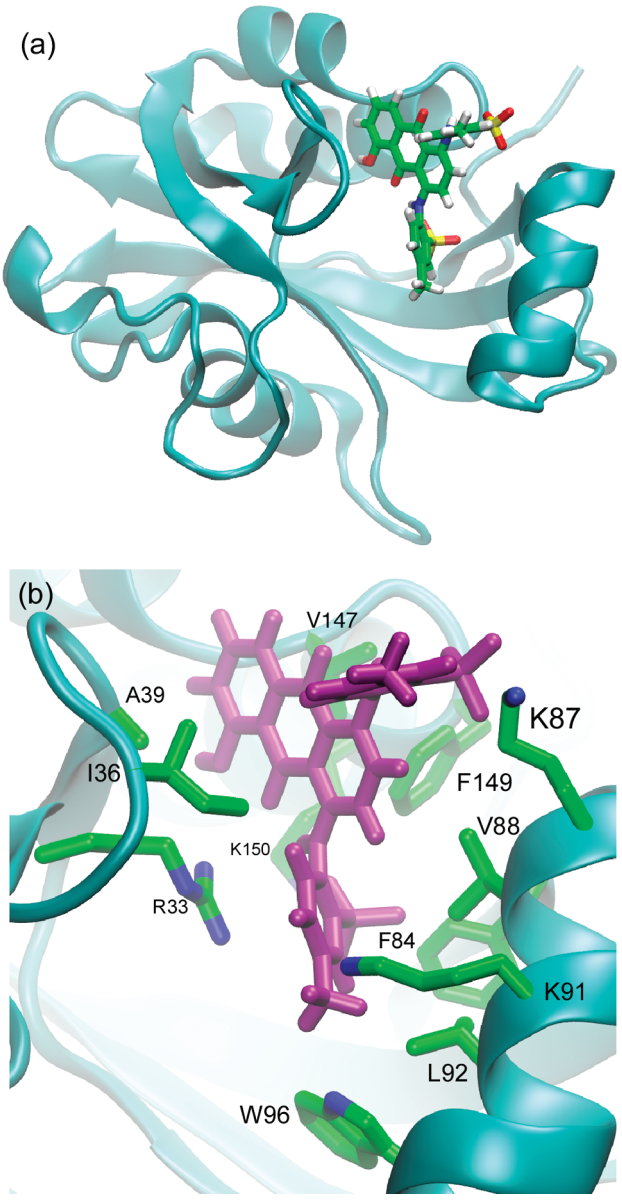

FIGURE 7: (a) Docked orientation of NSC51531 bound to lupin Ap_4A hydrolase. NSC51531 is shown in stick representation while the protein is represented in ribbon form (in cyan). The orientation is the same as presented in Figure 4. (b) Active site of Ap_4A hydrolase with NSC51531 (in purple) bound. Side-chain atoms of the residues in contact with the ligand are shown (C, green; N, nitrogen; O, oxygen).

hydrolase (*36*) have revealed a different mode of binding of substrate compared to the lupin hydrolase. Neither the human nor *C. elegans* enzymes possess the mobile helix II observed in lupin Ap_4A hydrolase. The side-chain groups of four residues on helix II, V88, K91, L92, and W96, contact ATP; these residues also contact NSC51531 in the predicted docked pose of the inhibitor. The side-chain groups of R33 and K150 of the lupin Ap_4A hydrolase engage the furan-linked phosphate of ATP; both of these residues are predicted to bind one of the sulfonates of NSC51531. Notably, no basic residues exist in the vicinity of R33 or K150 in the human Ap_4A hydrolase.

The dichotomy between the structures of lupin and human Ap_4A hydrolase, particularly in the ligand-binding site, suggests that the lead reported here presents a reasonable starting point for the design of specific inhibitors of bacterial pathogen Ap_4A hydrolases. Such inhibitors might also provide a valuable research tool for understanding the roles of Ap_4A in bacterial pathogenesis or in other mechanisms. NSC51531 shows no adverse effects against human fibroblasts up to concentrations of 100 μM, intimating tolerance to this class of compound and the applicability for drug development.

Neither of the structural analogues NSC86169 or NSC300513 contain a sulfonate group; the role of the sulfonate groups in engaging basic residues in the ligand-binding site of Ap_4A hydrolase offers a clear explanation for the decreased binding affinity of these compounds. It is reassuring, also, that these compounds were not rated highly in the *in silico* screening procedure.

CONCLUSIONS

In silico screening has been used to identify several novel inhibitors of lupin Ap_4A hydrolase. Two of these compounds, possessing a 1,4-diaminoanthracene-9,10-dione core, bind with a K_i of 1−3 μM, as determined through isothermal titration calorimetry. NMR chemical shift analysis of the compound exhibiting the highest affinity for the enzyme indicates that the interaction is in the intermediate exchange regime, consistent with a low micromolar affinity. Perturbations of the peak intensities in the NMR spectra were observed to cluster around the substrate-binding site, demonstrating that the inhibitor bound specifically in this site. Sulfonate groups on the inhibitors appear to be necessary for the observed affinity and likely substitute for the phosphate groups of the substrate.

The *in silico* screening protocol applied here has been exceptionally successful. The highest ranked compound considered suitable for assaying exhibited tight binding to the enzyme. Of the six compounds selected from the original database of ~120000 compounds three exhibited inhibitory effects. Half the compounds assayed exhibited poor solubility, and an alternative accurate method for the prediction of solubility (in DMSO mixtures) is required to improve the rate of recovery of active compounds.

Ap_4A hydrolases are expressed ubiquitously across all cellular systems. NSC51531 exhibits binding in the substrate-binding site of lupin Ap_4A hydrolase, whereas for the human form the interaction is nonspecific. Thus, the 1,4-diaminoanthracene-9,10-dione core may serve as a useful scaffold for future design of specific inhibitors of the plant/bacterial family of Ap_4A hydrolases that capitalize on the differences in ligand binding sites between animal and plant/bacterial forms of the enzymes. We have demonstrated here the ability to identify inhibitors of this group of enzymes. It remains to determine whether Ap_4A hydrolases are critical for parasite survival to validate this as a target for therapeutic intervention. The compounds identified here will be valuable for determining the importance of Ap_4A hydrolases in pathogenesis.

REFERENCES

1. McLennan, A. G., Barnes, L. D., Blackburn, G. M., Brenner, C., Guranowski, A., Miller, A. D., Rovira, J. M., Rotlan, P., Soria, B., Tanner, J. A., and Sillero, A. (2001) Recent progress in the study of the intracellular functions of diadenosine polyphosphates. *Drug Dev. Res. 52*, 249–259.
2. Hoyle, C. H. V., Hilderman, R. H., Pintor, J. J., Schluter, H., and King, B. F. (2001) Diadenosine polyphosphates as extracellular signal molecules. *Drug Dev. Res. 52*, 260–273.
3. Carmi-Levy, I., Yannay-Cohen, N., Kay, G., Razin, E., and Nechushtan, H. (2008) Diadenosine teraphosphate hydrolase is part

of the transcriptional regulation network in immunologically activated mast cells. *Mol. Cell. Biol. 28*, 5777–5784.
4. Cartwright, J. L., Britton, P., Minnick, M. F., and McLennan, A. G. (1999) The IalA invasion gene of *Bartonella bacilliformis* encodes a (de)nucleoside polyphosphate hydrolase of the MutT motif family and has homologs in other invasive bacteria. *Biochem. Biophys. Res. Commun. 256*, 474–479.
5. McLennan, A. G. (1999) The MutT motif family of nucleotide phosphohydrolases in man and human pathogens. *Int. J. Mol. Med. 4*, 79–89.
6. Mitchell, S. J., and Minnick, M. F. (1995) Characterisation of a two gene locus from *Bartonella bacilliformis* associated with the ability to invade human erythrocytes. *Infect. Immun. 63*, 1552–1562.
7. Guranowski, A. (2000) Specific and nonspecific enzymes involved in the catabolism of mononucleoside and dinucleoside polyphosphates. *Pharmacol. Ther. 87*, 117–139.
8. Guranowski, A., Brown, P., Ashton, P. A., and Blackburn, G. M. (1994) Regiospecificity of the hydrolysis of diadenosine polyphosphates catalyzed by three specific pyrophosphohydrolases. *Biochemistry 33*, 235–240.
9. Bessman, M. J., Frick, D. N., and O'Handley, S. F. (1996) The MutT proteins or "nudix" hydrolases, a family of versatile, widely distributed, "housecleaning" enzymes. *J. Biol. Chem. 271*, 25059–25062.
10. Fletcher, J. I., Swarbrick, J. D., Maksel, D., Gayler, K. R., and Gooley, P. R. (2002) The structure of Ap(4)A hydrolase complexed with ATP-MgF_x reveals the basis of substrate binding. *Structure 10*, 205–213.
11. Guranowski, A., Biryukov, A., Tarussova, N. B., Khomutov, R. M., and Jakubowski, H. (1987) Phosphonate analogues of diadenosine 5′,5‴-P1,P4-tetraphosphate as substrates or inhibitors of procaryotic and eucaryotic enzymes degrading dinucleoside tetraphosphates. *Biochemistry 26*, 3425–3429.
12. Guranowski, A., Starzynska, E., McLennan, A. G., Baraniak, J., and Stec, W. J. (2003) Adenosine-5′-O-phosphorylated and adenosine-5′-O-phosphorothioylated polyols as strong inhibitors of (symmetrical) and (asymmetrical) dinucleoside tetraphosphatases. *Biochem. J. 373*, 635–640.
13. Guranowski, A., Starzynska, E., Pietrowska-Borek, M., Jemielity, J., Kowalska, J., Darzynkiewicz, E., Thompson, M. J., and Blackburn, G. M. (2006) Methylene analogues of adenosine 5′-tetraphosphate. Their chemical synthesis and recognition by human and plant mononucleoside tetraphosphates and dinucleoside tetraphosphates. *FEBS J. 273*, 829–838.
14. Rotllan, P., Rodriguez-Ferrer, C. R., Asensio, A. C., and Oaknin, S. (1998) Potent inhibition of specific diadenosine polyphosphate hydrolases by suramin. *FEBS Lett. 429*, 143–146.
15. Ewing, T. J., Makino, S., Skillman, A. G., and Kuntz, I. D. (2001) DOCK 4.0: search strategies for automated molecular docking of flexible molecule databases. *J. Comput.-Aided Mol. Des. 15*, 411–428.
16. Pearlman, R. S., Rusinko, A., Skell, J. M., and Balducci, R. Concord 4.0.2, University of Texas, Austin, TX; distributed by Tripos Inc., St. Louis, MO.
17. Wang, R. X., Liu, L., Lai, L. H., and Tang, Y. Q. (1998) SCORE: A new empirical method for estimating the binding affinity of a protein-ligand complex. *J. Mol. Model. 4*, 379–394.
18. Muegge, I., and Martin, Y. C. (1999) A general and fast scoring function for protein-ligand interactions: a simplified potential approach. *J. Med. Chem. 42*, 791–804.
19. Eldridge, M. D., Murray, C. W., Auton, T. R., Paolini, G. V., and Mee, R. P. (1997) Empirical scoring functions: I. The development of a fast empirical function to estimate the binding affinity of ligands in receptor complexes. *J. Comput.-Aided Mol. Des. 11*, 425–445.
20. Murray, C. W., Auton, T. R., and Eldridge, M. D. (1998) Empirical scoring functions: II. The testing of an empirical scoring function for the prediction of ligand-receptor binding affinities and the use of Bayesian regression to improve the quality of the model. *J. Comput.-Aided Mol. Des. 12*, 503–519.
21. DeWitte, R. S., and Shanhnovich, E. I. (1996) SMoG: de novo design method based on simple, fast, and accurate free energy estimates. 1. Methodology and supporting evidence. *J. Am. Chem. Soc. 118*, 11733–11744.
22. DeWitte, R. S., Ishchenko, A. V., and Shanhnovich, E. I. (1997) SMoG: de novo design method based on simple, fast, and accurate free energy estimates. 2. Case studies in molecular design. *J. Am. Chem. Soc. 119*, 4608–4617.
23. Morris, G. M., Goodsell, D. S., Halliday, R. S., Huey, R., Hart, W. E., Belew, R. K., and Olsen, A. J. (1998) Automated docking using a Lamarckian genetic algorithm and an empirical binding free energy function. *J. Comput. Chem. 19*, 1639–1162.
24. Wang, R., Lu, Y., and Wang, S. (2003) Comparative evaluation of 11 scoring functions for molecular docking. *J. Med. Chem. 46*, 2287–2303.
25. Wang, R., and Wang, S. (2001) How does consensus scoring work for virtual library screening? An idealized computer experiment. *J. Chem. Inf. Comput. Sci. 41*, 1422–1426.
26. Wang, R., Fu, Y., and Lai, L. (1997) A new atom-additive method for calculating partition coefficients. *J. Chem. Inf. Comput. Sci. 37*, 615–621.
27. Todd, M. J., and Gomez, J. (2001) Enzyme kinetics determined using calorimetry: A general assay for enzyme activity?. *Anal. Biochem. 296*, 179–187.
28. Swarbrick, J. D., Bashtannyk, T., Maksel, D., Zhang, X. R., Blackburn, G. M., Gayler, K. R., and Gooley, P. R. (2000) The three-dimensional structure of the nudix enzyme diadenosine tetraphosphate hydrolase from *Lupinus angustifolius* L. *J. Mol. Biol. 302*, 1165–1177.
29. Swarbrick, J. D., Buyya, S., Gundawardana, D., Galyer, K. R., McLennan and, A. G., and Gooley, P. R. (2005) Structure and substrate binding mechanism of human Ap_4A hydrolase. *J. Biol. Chem. 280*, 8471–8481.
30. Delaglio, F., Grzesiek, S., Vuister, G. W., Zhu, G., Pfeifer, J., and Bax, A. (1995) NMRPipe: a multidimensional spectral processing system based on UNIX pipes. *J. Biomol. NMR 6*, 277–293.
31. Bartels, Ch., Xia, T.-H., Billeter, M., Guntert, P., and Wuthrich, K. (1995) The program XEASY for computer-supported NMR spectral analysis of biological macromolecules. *J. Biomol. NMR 5*, 1–10.
32. Kedzierski, L., Curtis, J. M., Kaminska, M., Jodynis-Liebert, J., and Murias, M. (2007) In vitro antileishmanial activity of resveratrol and its hydroxylated analogues against *Leishmania major* promastigotes and amastigotes. *Parasitol. Res. 102*, 91–97.
33. Maksel, D., Gooley, P. R., Swarbrick, J. D., Guranowski, A., Gange, C., Blackburn, G. M., and Gayler, K. R. (2001) Characterization of active-site residues in diadenosine tetraphosphate hydrolase from *Lupinus angustifolius*. *Biochem. J. 357*, 399–405.
34. Wemmer, D. E., and Williams, P. G. (1994) Use of magnetic resonance in probing ligand-macromolecule interactions. *Methods Enzymol. 239*, 739–767.
35. Swarbrick, J. D., Guranowski, A., Gange, C., Blackburn, G. M., and Gayler, K. R. (2001) Characterization of active-site residues in diadenosine tetraphosphate hydrolase from *Lupinus angustifolius*. *Biochem. J. 357*, 399–405.
36. Bailey, S., Sedelnikova, S. E., Blackburn, G. M., Abdelghany, H. M., Baker, P. J., McLennan, A. G., and Rafferty, J. B. (2002) The crystal structure of diadenosine tetraphosphate hydrolase from *Caenorhabditis elegans* in free and binary complex forms. *Structure 10*, 589–600.